PHYSICAL REVIEW B **92**, 081104(R) (2015)

Beyond the *GW* approximation: A second-order screened exchange correction

Xinguo Ren,[1,2,3] Noa Marom,[4] Fabio Caruso,[2,5] Matthias Scheffler,[2] and Patrick Rinke[2,6]

[1]*Key Laboratory of Quantum Information, University of Science and Technology of China, Hefei 230026, China*

[2]*Fritz-Haber-Institut der Max-Planck-Gesellschaft, Faradayweg 4-6, D-14195 Berlin, Germany*

[3]*Synergistic Innovation Center of Quantum Information and Quantum Physics, University of Science and Technology of China, 230026 Hefei, China*

[4]*Department of Physics and Engineering Physics, Tulane University, New Orleans, Louisiana 70118, USA*

[5]*Department of Materials, University of Oxford, Parks Road, OX1 3PH, United Kingdom*

[6]*COMP/Department of Applied Physics, Aalto University, P.O. Box 11100, Aalto FI-00076, Finland*

(Received 30 November 2014; revised manuscript received 22 April 2015; published 7 August 2015)

Motivated by the recently developed renormalized second-order perturbation theory for ground-state energy calculations, we propose a second-order screened exchange correction (SOSEX) to the *GW* self-energy. This correction follows the spirit of the SOSEX correction to the random-phase approximation for the electron correlation energy and can be clearly represented in terms of Feynman diagrams. We benchmark the performance of the perturbative G_0W_0+SOSEX scheme for a set of molecular systems, including the G2 test set from quantum chemistry as well as benzene and tetracyanoethylene. We find that G_0W_0+SOSEX improves over G_0W_0 for the energy levels of the highest occupied and lowest unoccupied molecular orbitals. In addition, it can resolve some of the difficulties encountered by the *GW* method for relative energy positions as exemplified by benzene where the energy spacing between certain valence orbitals is severely underestimated.

DOI: 10.1103/PhysRevB.92.081104 PACS number(s): 71.15.Mb, 31.15.ae, 31.15.vq, 82.37.−j

The energy gain from adding an electron to, or the cost of removing an electron from a molecule, a nanostructure, or a solid is a fundamental property, which can be measured by experimental techniques such as photoemission or inverse photoemission spectroscopy. The first-principles theory of choice for describing such charged excitations in solid-state physics has been many-body perturbation theory in the *GW* approximation [1], due to its balance between accuracy and computational expense [2–4]. Recently, the *GW* approach has also increasingly been applied to molecules and nanosystems [5–12].

An accurate determination of single-particle excitation energies is indispensable in many areas of chemistry, physics, materials science, and nanoscience. However, despite the success of the *GW* approach, several challenges remain. While some of *GW*'s shortcomings can be attributed to the starting-point dependence [11,13–15] of the common perturbative (G_0W_0) scheme, others persist also in self-consistent schemes [10,16]. For example, in solids, the binding energies of semicore states tend to be underestimated [17,18], whereas band gaps of polar materials are often severely overestimated [19]. Also an assessment of *d*- and *f*-electron compounds is only just emerging with partial success [20–23]. For finite systems, G_0W_0 based on a Perdew-Burke-Ernzerhof hybrid functional (PBE0) [24] reference yields excellent vertical ionization energies (IEs) for molecules with an average deviation from experiment of only 3% [9,11,12,15]. However, relative energy differences in the full spectrum are not always this accurate. A good example is the benzene molecule, for which the energy separation of the two states just below the highest-occupied-molecular-orbital (HOMO) is considerably underestimated in *GW* ($\sim$0.1 eV compared to $\sim$0.6 eV in experiment) [15]. For molecules with lone pair orbitals, the energy ordering of the first few valence orbitals can be incorrect [15], whereas for some acceptor molecules with positive electron affinities (EAs), e.g., tetracyanoethylene (TCNE), *GW* tends to overestimate the EAs substantially, irrespective of the starting point or the self-consistent scheme. These are just a few examples to illustrate the need to go beyond the *GW* approximation.

Beyond-*GW* schemes, so-called "vertex corrections," have a long history [25–30]. However, simple, computationally efficient vertex corrections [25] have almost no effect on the *GW* description, while more elaborate schemes are computationally so involved that they have only been applied to the homogeneous electron gas [26,29], the Hubbard molecule [31], or simple solids such as silicon or argon [25,27,28,32]. Thus, there is currently no generally accepted way to go beyond the *GW* approach for real solids, molecules, or nanostructures. Here, we focus on finite systems and present a self-energy correction to *GW* that derives rigorously from many-body perturbation theory, is computationally tractable, and improves on *GW* in almost all the cases mentioned above.

We propose to go beyond *GW* by adding a subset of higher-order exchange-type diagrams. This additional self-energy term is inspired by the renormalized second-order perturbation theory (rPT2) [33] for the electron correlation energy that some of us have developed recently. rPT2 improves on the random-phase approximation (RPA) [34–36] with second-order screened exchange (SOSEX) [37,38] and a renormalized single-excitation term (rSE) [39]. This yields a much more balanced description than RPA alone or RPA combined with either SOSEX or rSE can achieve [33]. The exchange-correlation diagrams in RPA are topologically identical to those of the (perturbative) G_0W_0 approach [40,41]. *GW* thus provides the corresponding self-energy to RPA. Here we demonstrate that, in a similar fashion, we can derive a self-energy that corresponds to the SOSEX term. The rSE term is automatically included and thus does not appear explicitly in the self-energy.

The RPA correlation energy can be computed as [42]

$$E_c^{\mathrm{RPA}} = \frac{1}{2}\sum_{ij,ab}\langle ij|ab\rangle T_{jb,ia}. \quad (1)$$

$T_{jb,ia}$ are the ring coupled-cluster doubles amplitudes and $\langle ij|ab\rangle$ the bare two-electron Coulomb integrals,

$$\langle ij|ab\rangle = \iint dx_1 dx_2 \frac{\psi_i^*(x_1)\psi_a(x_1)\psi_j^*(x_2)\psi_b(x_2)}{|\mathbf{r}_1-\mathbf{r}_2|}. \quad (2)$$

Here $x=(\mathbf{r},\sigma)$ is a combined spatial-spin variable, and i,j and a,b refer to occupied and unoccupied Kohn-Sham single-particle spin orbitals, respectively. The RPA+SOSEX correlation energy can then be obtained by *antisymmetrizing* the Coulomb integrals in Eq. (1) [37], i.e., $\langle ij|ab\rangle \rightarrow \langle ij||ab\rangle = \langle ij|ab\rangle - \langle ij|ba\rangle$.

To apply the same strategy to the self-energy, we separate the GW self-energy into its exact exchange and the remaining correlation part $\Sigma^{GW} = \Sigma_{\mathrm{x}} + \Sigma_{\mathrm{c}}^{GW}$. The Σ_{c}^{GW} term is then given by

$$\Sigma_{\mathrm{c}}^{GW}(1,2) = iG(1,2)[W(1,2)-v(1,2)], \quad (3)$$

where G is the Green's function of the interacting electron system, v is the bare Coulomb interaction, and W is the screened Coulomb interaction. The numbers are a shorthand notation for combined spatial, spin, and time variables [i.e., $1=(\mathbf{r}_1,\sigma_1,t_1)$]. Here, as usual, W is evaluated at the RPA level, i.e.,

$$W(1,2) = v(1,2) + \int d3d4 v(1,3)\chi_0(3,4)W(4,2), \quad (4)$$

where χ_0 is the irreducible polarizability,

$$\chi_0(1,2) = -iG(1,2)G(2,1). \quad (5)$$

Σ_{c}^{GW} can thus be rewritten as

$$\Sigma_{\mathrm{c}}^{GW}(1,2) = \int d3d4\, G(1,2)v(1,3)G(3,4)G(4,3)W(4,2), \quad (6)$$

which is illustrated by Feynman diagrams in Fig. 1(a). The diagrams reveal that Σ_{c}^{GW} arises from screened second-order direct (Coulomb) interactions.

The key step comes next: By exchanging the connection between the Green's function and the (bare and screened) Coulomb interaction lines, we arrive at a second-order screened exchange diagram, which we call the SOSEX self-energy

$$\Sigma_{\mathrm{c}}^{\mathrm{SOSEX}}(1,2) = -\int d3d4\, G(1,4)v(1,3)G(4,3)G(3,2)W(4,2). \quad (7)$$

The procedure is illustrated diagrammatically in Fig. 1(b) [43].

Traditionally, perturbation theories have been mostly carried out by considering Σ_{xc} to be a functional of either G and W or a functional of G and v. The diagrammatic representation of Σ_{c}^{GW} in Fig. 1(a) suggests that one may combine both options, which makes the construction of diagrams more flexible, but carries the danger of double counting. By further expanding W in terms of v, we ensured that no term in our theory is counted more than once. The Σ_{c}^{GW} and $\Sigma_{\mathrm{c}}^{\mathrm{SOSEX}}$ diagrams are the only two nontrivial self-energy diagrams which can be constructed with one v line and one W line, in analogy to the conventional second-order self-energy that is given in terms of the two *bare* Coulomb lines [9,44,45].

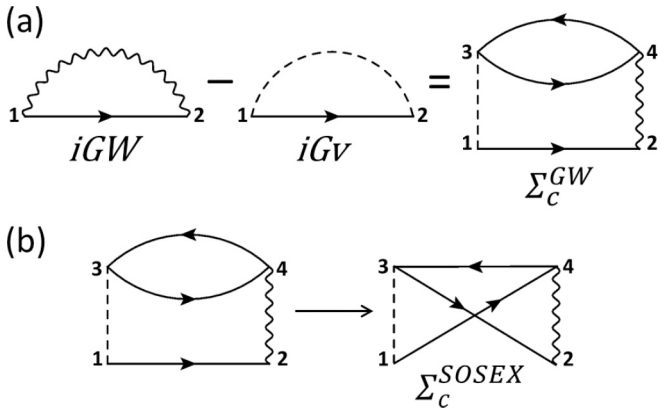

FIG. 1. (a) Feynman diagram for the correlation part of the GW self-energy (Σ_{c}^{GW}); (b) diagrammatic illustration of obtaining the SOSEX self-energy from Σ_{c}^{GW} by interchanging the Green's function lines. Solid lines, dashed lines, and wiggly lines represent the Green's function, the bare Coulomb, and the screened Coulomb interaction, respectively.

The construction of different diagrammatic series is guided by different principles, e.g., conservation of certain properties [46,47], positivity of the spectral function [48] or size consistency [45]. Our SOSEX self-energy in Eq. (7) can be viewed as a functional derivative of a SOSEX-type correlation energy with respect to the Green's function, while keeping the screened Coulomb interaction fixed. This SOSEX-type correlation energy is, however, different from the coupled-cluster SOSEX [37] and the adiabatic-connection SOSEX [49] discussed in the literature. In future work, we will put our double expansion in v and W on a more rigorous footing [50].

It should be noted that the SOSEX correction to GW proposed here is different from a straightforward second-order expansion in terms of W, as originally formulated by Hedin [1], for which the SOSEX self-energy diagram [cf. Fig. 1(b)] contains two screened Coulomb lines. If one expands W in terms of v for both self-eneriges, one will find the two approaches are identical to leading order (second order in v), but differ for higher orders. For example, at third order in v, the SOSEX self-energy is only half of Hedin's second-order self-energy in W, because the latter contains two topologically equivalent diagrams while the former only picks up one of them. The SOSEX self-energy diagrams are a subset of those included in Hedin's self-energy, and hence can be considered as an approximation to the latter. Compared to the SOSEX self-energy proposed here, a full treatment of the second-order self-energy in W is numerically much more challenging because of the presence of a double frequency integration. Historically, it was first examined numerically for silicon by Bobbert and van Haeringen [27] with a plasmon-pole approximation for W, but no appreciable change to G_0W_0 was observed. Very recently, Grüneis *et al.* [30] implemented an approximate version of this scheme using static W's and found

that the ionization energies and d-electron binding energies of solids were improved.

Returning to the rPT2 analogy, rPT2 contains a third term that arises from single excitations [33]. Close inspection reveals that the single-excitation contributions as included in rSE only leads to improper self-energy diagrams [51], i.e., merely trivial repetitions of the irreducible self-energy part. As demonstrated in the Supplemental Material [51], the irreducible part of the rSE self-energy is nothing but the difference between the exact-exchange self-energy and the Kohn-Sham (KS) exchange-correlation potential, $\Delta v = \Sigma_x - v_{\rm xc}^{\rm KS}$, which is already included in normal G_0W_0 calculations. We thus conclude that the sum of Σ^{GW} and $\Sigma_c^{\rm SOSEX}$ corresponds to a proper renormalized second-order perturbation theory for the self-energy.

In analogy to the G_0W_0 method, we have implemented GW+SOSEX in a perturbative way, denoted as G_0W_0+SOSEX in the following. In terms of a set of single-particle spin orbitals $\psi_p(x)$ (with energies ϵ_p) for which G_0 is diagonalized, we have

$$G_0(x_1,x_2;i\omega) = \sum_p \frac{\psi_p(x_1)\psi_p^*(x_2)}{i\omega - \epsilon_n}. \tag{8}$$

For numerical simplicity we work on the imaginary frequency axis, and the results will be analytically continued to the real axis at the end. Using (6), (7), and (8), the diagonal matrix elements of $\Sigma_c^{G_0W_0+\rm SOSEX}$ within the set of orbitals $\{\psi_p(x)\}$ are given by

$$\begin{aligned}&\left[\Sigma_{\rm c}^{GW+\rm SOSEX}\right]_{pp}(i\omega)\\ &\quad= \langle\psi_p|\Sigma_{\rm c}^{GW} + \Sigma_{\rm c}^{\rm SOSEX}(i\omega)|\psi_p\rangle\\ &\quad= -\frac{1}{2\pi}\int_{-\infty}^{\infty} d\omega' \sum_{qrs} \frac{(f_q - f_r)\langle pr||qs\rangle\langle qs|W(i\omega')|pr\rangle}{(i\omega + i\omega' - \epsilon_s)(i\omega' + \epsilon_q - \epsilon_r)},\end{aligned} \tag{9}$$

where $\langle qs|W(i\omega')|pr\rangle$ are the two-electron integrals for the screened Coulomb interaction. In Eq. (9), the summation over spin-orbital indices p,q,r runs over both occupied and unoccupied states, and f_q and f_r are Fermi occupation factors. In this work we only consider closed-shell molecules, and hence $f_q = 1$ for occupied states, and 0 for unoccupied states.

Equation (9) has been implemented in the local-orbital based, all-electron Fritz Haber Institute *ab initio molecular simulations* (FHI-aims) code package [9,52]. In FHI-aims two-electron Coulomb integrals are evaluated using the resolution-of-identity (RI) technique. The implementation details for correlated methods (including RPA, RPA+SOSEX, and GW) have been documented in Refs. [9,33], which our GW+SOSEX implementation follows closely. Computationally, a standard RI implementation of Eq. (9) using canonical molecular orbitals scales as $O(N^5)$ with respect to the system size N. Ways to reduce the scaling are foreseeable if one exploits the locality of the atomic orbitals and the Green's function.

Next, we demonstrate the performance of G_0W_0+SOSEX. We use the notation @DF to denote the density functional (DF) starting point that the perturbative calculation is based on [e.g., G_0W_0@PBE refers to a Perdew-Burke-Ernzerhof (PBE)

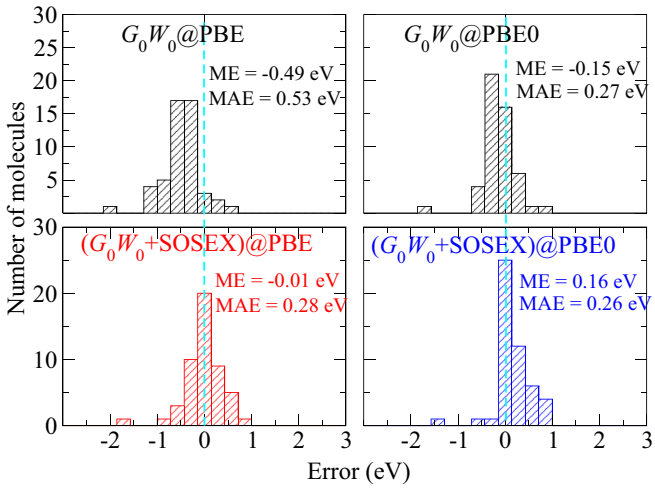

FIG. 2. (Color online) Histograms of the vIE error distribution of 50 atoms and small molecules [9]. Here *tier* 4 was augmented by the diffuse functions from the Gaussian aug-cc-pV5Z basis set [55].

[53] based G_0W_0 calculation]. Unless otherwise stated, the high-quality *tier* 4 FHI-aims-2009 basis sets [52] are used in the calculations below [54].

We first check how well GW+SOSEX performs for ionization energies, considering a subset of 50 molecules from the G2 test set [56]. The vertical IEs (vIEs) used here as reference are those obtained by the G2 theory itself [56], corrected by the difference between adiabatic ionization energies (aIEs) and vIEs given by experiment:

$$E^{\rm vIE}({\rm Ref.}) = E^{\rm aIE}({\rm G2}) + E^{\rm vIE}({\rm Expt.}) - E^{\rm aIE}({\rm Expt.}). \tag{10}$$

The error distribution of the vIEs is presented in Fig. 2 for G_0W_0 and G_0W_0+SOSEX, based on both PBE and PBE0. The G_0W_0 results were already presented in Ref. [9] where it was shown that G_0W_0@PBE systematically underestimates vIEs, whereas G_0W_0@PBE0 yields results that are in good agreement with experiment on average. This behavior does not change when comparing to the reference values obtained from the G2 theory, as can be seen from Fig. 2. Adding the SOSEX correction, the aIEs are systematically increased, and now (G_0W_0+SOSEX)@PBE yields a vanishingly small mean error (ME) of only -0.01 eV, and a mean absolute error (MAE) of 0.28 eV that is comparable to G_0W_0@PBE0. Conversely, (G_0W_0+SOSEX)@PBE0 has a MAE of 0.26 eV, comparable to both (G_0W_0+SOSEX)@PBE and G_0W_0@PBE0. The ME is now 0.16 eV, which indicates that (G_0W_0+SOSEX)@PBE0 on average slightly overestimates vIEs, in contrast to (G_0W_0+SOSEX)@PBE that slightly underestimates vIEs. Not surprisingly, as a purturbative treatment, G_0W_0+SOSEX still shows noticeable dependence on the reference orbitals. However, on average this dependence is not as significant as the G_0W_0 case, as measured by the respective ME differences. In the Supplemental Material [51] we further present G_0W_0+SOSEX benchmark results for two other subsets of G2, and compare them to reference results obtained with coupled-cluster theory with single, double, and perturbative triple truncations [CCSD(T)]. The message from these additional tests is the same as conveyed in Fig. 2.

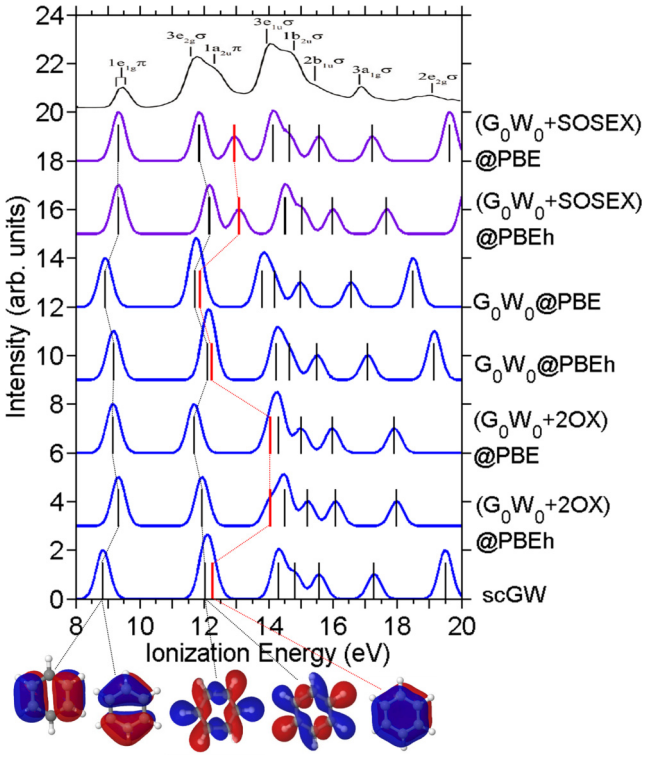

FIG. 3. (Color online) Quasiparticle energy spectra of the benzene molecule [64], obtained with different GW based schemes. The experimental photoemission spectrum is taken from Ref. [62]. The short vertical lines below the peaks mark the positions of the energy levels (obtained as delta peaks) before broadening with a 0.3 eV Gaussian (with thick lines corresponding to twofold degenerate and thin lines to nondegenerate states).

The benzene molecule is our next example. The HOMO is a twofold degenerate π state (e_{1g} representation), whose G_0W_0 energy has been calculated by various groups [9,57–59]. The general agreement of G_0W_0 and the experimental vIE is satisfactory (cf. Fig. 3). However, our real interest lies in the energy spacing of the next two states below the HOMO (denoted as HOMO-1 and HOMO-2, respectively). These are the twofold degenerate $e_{2g}(\sigma)$ and the nondegenerate $a_{1u}(\pi)$ states [60,61]. The exact energy spacing between these two peaks varies slightly between different experiments [61–63], but is larger than 0.5 eV in all cases. However, in all G_0W_0 as well as in self-consistent GW (scGW) calculations [10] this separation is vanishingly small ($\sim$0.1 eV). The two peaks merge into one when a Gaussian broadening of 0.3 eV is applied as in Fig. 3. Most importantly, the splitting in G_0W_0 is independent of the starting point and therefore does not depend on the self-interaction error that might be present in the preceding mean-field calculation. We thus conclude that the significant underestimation of the $e_{2g}(\sigma)$-$a_{2u}(\pi)$ splitting in benzene is an intrinsic GW error that requires a correlation treatment beyond GW.

Figure 3 shows that the addition of a bare second-order exchange term (G_0W_0+2OX) increases the splitting of the two peaks [15]. Unfortunately, G_0W_0+2OX overshoots, leading to an energy spacing of $\sim$2 eV. Screening the second-order exchange term, as in the G_0W_0+SOSEX scheme, moves the a_{2u} peak back. Now the $e_{2g}(\sigma)$-$a_{2u}(\pi)$ separation is $\sim$1 eV, which although not in perfect agreement with experiment, is a significant improvement upon GW.

The difficulty that GW encounters for benzene can be understood in terms of the delicate balance between the π-π (i.e., HOMO and HOMO-2) and the π-σ splitting (i.e., HOMO and HOMO-1). The HOMO and the HOMO-2 are both bonding π states that derive from the p_z orbital of the C atoms. However, their nodal structures are different: the lower $a_{2u}(\pi)$ state has no nodes, whereas the higher $e_{1g}(\pi)$ states have two nodes. The HOMO-1 state, on the other hand, exhibits a completely different σ bonding character arising from the $p_{x/y}$ orbitals of the C atoms. Describing the relative energy positions of these different orbitals is a challenging task. Although GW improves the KS spectrum in general, the self-screening problem of GW [65,66] affects the relative energy positions for orbitals that have drastically different bonding characters. Figure 3 illustrates that the higher-order exchange contribution controls the magnitude of the $e_{2g}(\sigma)$-$a_{2u}(\pi)$ splitting in benzene and that GW+SOSEX captures the essential physics that is missing in GW. Predicting relative energies accurately is of paramount importance for the level alignment at heterointerfaces as found in microelectronics, organic electronics, and at hybrid interfaces. We thus expect GW+SOSEX to play a significant role for such systems in the future.

The third example we consider here is the TCNE molecule—an excellent electron acceptor because of its large EA value, which is a highly desired property in certain electronic devices. In Fig. 4 we present several GW spectra

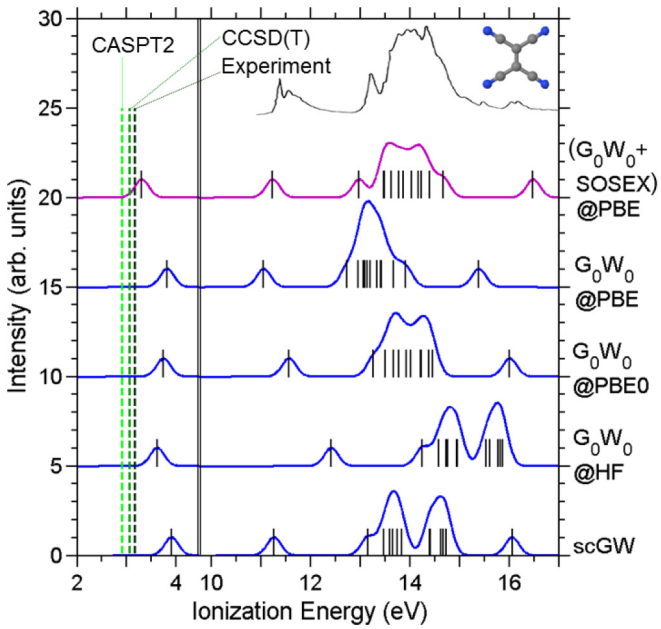

FIG. 4. (Color online) Quasiparticle spectra of TCNE obtained with different GW based schemes, in comparison to the experimental photoemission spectrum [67]. The positions of the first peaks on the left correspond to the vertical EA values, which are separated by the double vertical lines from the occupied states. Vertical dashed lines mark the experimental [68], the CCSD(T) [69], and the CASPT2 [70] EAs.

for TCNE in comparison to the experimental photoemission data [67]. The vertical EA (vEA) values of 3.05 eV obtained from CCSD(T) [69] and 2.91 eV from the complete active space method with a second-order perturbation (CASPT2) [70], as well as the experimental adiabatic EA value (3.16) are indicated by vertical dashed lines. We observe that all GW methods significantly overestimate the EA, even G_0W_0@HF, which usually yields the lowest unoccupied molecular orbital with the highest energy (smallest vEA). (G_0W_0+SOSEX)@PBE improves on G_0W_0@HF by more than 0.3 eV, reducing vEA from 3.61 to 3.30 eV. Moreover, we note that the improved description of G_0W_0+SOSEX for the unoccupied states does not deteriorate the occupied states. (G_0W_0+SOSEX)@PBE also yields the best valence spectrum.

To summarize, we have proposed a GW+SOSEX scheme for self-energy calculations. It goes systematically beyond the GW approximation and has a clear diagrammatic representation. We note that a perturbative expansion may appear intuitively clear and systematic. However, it always also carries a subjective component. Thus the final proof of the quality of such expansion is only provided by comparing to (essentially) exact results. This is the stratgey taken in the present work. Extensive benchmark calculations were carried out, which show that G_0W_0+SOSEX gives vIEs of atoms and small molecules in excellent agreement with the best theoretical reference values. G_0W_0+SOSEX also improves on GW for the relative energy position of molecular orbitals in difficult cases such as benzene and for electron affinities of strong acceptors such as TCNE, which G_0W_0 consistently overestimates.

Work at University of Science and Technology of China was supported by the National Natural Science Foundation of China Award No. 11374276. Work at Tulane University was supported by the Louisiana Alliance for Simulation-Guided Materials Applications (LA-SiGMA), funded by the National Science Foundation (NSF) Award No. EPS-1003897. This research has also been supported by the Academy of Finland through its Centres of Excellence Program (Project No. 251748).

[1] L. Hedin, Phys. Rev. **139**, A796 (1965).
[2] M. S. Hybertsen and S. G. Louie, Phys. Rev. B **34**, 5390 (1986).
[3] F. Aryasetiawan and O. Gunnarsson, Rep. Prog. Phys. **61**, 237 (1998).
[4] P. Rinke, A. Qteish, J. Neugebauer, and M. Scheffler, Phys. Status Solidi B **245**, 929 (2008).
[5] C. Rostgaard, K. W. Jacobsen, and K. S. Thygesen, Phys. Rev. B **81**, 085103 (2010).
[6] X. Blase, C. Attaccalite, and V. Olevano, Phys. Rev. B **83**, 115103 (2011).
[7] D. Foerster, P. Koval, and D. Sánchez-Portal, J. Chem. Phys. **135**, 074105 (2011).
[8] C. Faber, I. Duchemin, T. Deutsch, C. Attaccalite, V. Olevano, and X. Blase, J. Mater. Sci. **47**, 7472 (2012).
[9] X. Ren, P. Rinke, V. Blum, J. Wieferink, A. Tkatchenko, A. Sanfilippo, K. Reuter, and M. Scheffler, New J. Phys. **14**, 053020 (2012).
[10] F. Caruso, P. Rinke, X. Ren, M. Scheffler, and A. Rubio, Phys. Rev. B **86**, 081102(R) (2012); **88**, 075105 (2013).
[11] F. Bruneval and M. A. L. Marques, J. Chem. Theory Comput. **9**, 324 (2013).
[12] M. J. van Setten, F. Weigend, and F. Evers, J. Chem. Theory Comput. **9**, 232 (2013).
[13] P. Rinke, A. Qteish, J. Neugebauer, C. Freysoldt, and M. Scheffler, New J. Phys. **7**, 126 (2005).
[14] F. Fuchs, J. Furthmüller, F. Bechstedt, M. Shishkin, and G. Kresse, Phys. Rev. B **76**, 115109 (2007).
[15] N. Marom, F. Caruso, X. Ren, O. T. Hofmann, T. Körzdörfer, J. R. Chelikowsky, A. Rubio, M. Scheffler, and P. Rinke, Phys. Rev. B **86**, 245127 (2012).
[16] M. van Schilfgaarde, T. Kotani, and S. Faleev, Phys. Rev. Lett. **96**, 226402 (2006).
[17] M. Rohlfing, P. Krüger, and J. Pollmann, Phys. Rev. B **57**, 6485 (1998).
[18] T. Miyake, P. Zhang, M. L. Cohen, and S. G. Louie, Phys. Rev. B **74**, 245213 (2006).
[19] S. Botti and M. A. L. Marques, Phys. Rev. Lett. **110**, 226404 (2013).
[20] H. Jiang, R. I. Gómez-Abal, P. Rinke, and M. Scheffler, Phys. Rev. B **82**, 045108 (2010).
[21] J. H. Richter, B. J. Ruck, M. Simpson, F. Natali, N. O. V. Plank, M. Azeem, H. J. Trodahl, A. R. H. Preston, B. Chen, J. McNulty *et al.*, Phys. Rev. B **84**, 235120 (2011).
[22] H. Jiang, P. Rinke, and M. Scheffler, Phys. Rev. B **86**, 125115 (2012).
[23] M. Gatti and M. Guzzo, Phys. Rev. B **87**, 155147 (2013).
[24] C. Adamo and V. Barone, J. Chem. Phys. **110**, 6158 (1999).
[25] R. Del Sole, L. Reining, and R. W. Godby, Phys. Rev. B **49**, 8024 (1994).
[26] E. L. Shirley, Phys. Rev. B **54**, 7758 (1996).
[27] P. A. Bobbert and W. van Haeringen, Phys. Rev. B **49**, 10326 (1994).
[28] F. Bruneval, F. Sottile, V. Olevano, R. Del Sole, and L. Reining, Phys. Rev. Lett. **94**, 186402 (2005).
[29] H. Maebashi and Y. Takada, Phys. Rev. B **84**, 245134 (2011).
[30] A. Grüneis, G. Kresse, Y. Hinuma, and F. Oba, Phys. Rev. Lett. **112**, 096401 (2014).
[31] P. Romaniello, F. Bechstedt, and L. Reining, Phys. Rev. B **85**, 155131 (2012).
[32] R. T. M. Ummels, P. A. Bobbert, and W. van Haeringen, Phys. Rev. B **57**, 11962 (1998).
[33] X. Ren, P. Rinke, G. E. Scuseria, and M. Scheffler, Phys. Rev. B **88**, 035120 (2013).
[34] D. Bohm and D. Pines, Phys. Rev. **92**, 609 (1953).
[35] H. Eshuis, J. E. Bates, and F. Furche, Theor. Chem. Acc. **131**, 1084 (2012).
[36] X. Ren, P. Rinke, C. Joas, and M. Scheffler, J. Mater. Sci. **47**, 7447 (2012).
[37] A. Grüneis, M. Marsman, J. Harl, L. Schimka, and G. Kresse, J. Chem. Phys. **131**, 154115 (2009).
[38] J. Paier, B. G. Janesko, T. M. Henderson, G. E. Scuseria, A. Grüneis, and G. Kresse, J. Chem. Phys. **132**, 094103 (2010); **133**, 179902 (2010).

[39] X. Ren, A. Tkatchenko, P. Rinke, and M. Scheffler, Phys. Rev. Lett. **106**, 153003 (2011).
[40] N. E. Dahlen and U. von Barth, Phys. Rev. B **69**, 195102 (2004).
[41] F. Caruso, D. R. Rohr, M. Hellgren, X. Ren, P. Rinke, A. Rubio, and M. Scheffler, Phys. Rev. Lett. **110**, 146403 (2013).
[42] G. E. Scuseria, T. M. Henderson, and D. C. Sorensen, J. Chem. Phys. **129**, 231101 (2008).
[43] The sign difference between Eq. (6) and Eq. (7) arises from the fact that the Feynman diagram for $\Sigma_c^{\mathrm{SOSEX}}$ contains no closed fermionic loop, while Σ_c^{GW} has one.
[44] A. L. Fetter and J. D. Walecka, *Quantum Theory of Many-Particle Systems* (McGraw-Hill, New York, 1971).
[45] A. Szabo and N. S. Ostlund, *Modern Quantum Chemistry: Introduction to Advanced Electronic Structure Theory* (McGraw-Hill, New York, 1989).
[46] G. Baym and L. P. Kadanoff, Phys. Rev. **124**, 287 (1961).
[47] C.-O. Almbladh, U. von Barth, and R. van Leeuwen, Int. J. Mod. Phys. B **13**, 535 (1999).
[48] G. Stefanucci, Y. Pavlyukh, A.-M. Uimonen, and R. van Leeuwen, Phys. Rev. B **90**, 115134 (2014).
[49] G. Jansen, R.-F. Liu, and J. G. Ángyán, J. Chem. Phys. **133**, 154106 (2010).
[50] It appears that the SOSEX self-energy is not a Φ- or Ψ-derivable theory [47], and one may then question its conserving property which is a relevant issue when running self-consistent calculations.
[51] See Supplemental Material at http://link.aps.org/supplemental/10.1103/PhysRevB.92.081104 for further details.
[52] V. Blum, F. Hanke, R. Gehrke, P. Havu, V. Havu, X. Ren, K. Reuter, and M. Scheffler, Comput. Phys. Commun. **180**, 2175 (2009).
[53] J. P. Perdew, K. Burke, and M. Ernzerhof, Phys. Rev. Lett. **77**, 3865 (1996); **78**, 1396 (1997).
[54] The convergence behavior of FHI-aims-2009 basis sets for G_0W_0-type calculations has been thoroughly investigated in Ref. [9].
[55] J. T. H. Dunning, J. Chem. Phys. **90**, 1007 (1989).
[56] L. A. Curtiss, P. C. Redfern, K. Raghavachari, and J. A. Pople, J. Chem. Phys. **109**, 42 (1998).
[57] P. Umari, G. Stenuit, and S. Baroni, Phys. Rev. B **81**, 115104 (2010).
[58] G. Samsonidze, M. Jain, J. Deslippe, M. L. Cohen, and S. G. Louie, Phys. Rev. Lett. **107**, 186404 (2011).
[59] S. Sharifzadeh, I. Tamblyn, P. Doak, P. Darancet, and J. Neaton, Eur. Phys. J. B **85**, 323 (2012).
[60] T. A. Carlson and C. P. Anderson, Chem. Phys. Lett. **10**, 561 (1971).
[61] T. A. Carlson, P. Gerard, M. O. Krause, F. A. Grimm, and B. P. Pullen, J. Chem. Phys. **86**, 6918 (1987).
[62] S.-Y. Liu, K. Alnama, J. Matsumoto, K. Nishizawa, H. Kohguchi, Y.-P. Lee, and T. Suzuki, J. Phys. Chem. A **115**, 2953 (2011).
[63] J. A. Sell and A. Kuppermann, Chem. Phys. **33**, 367 (1978).
[64] The PBE-relaxed (with *tier* 2 basis) geometry is used in the calculation.
[65] W. Nelson, P. Bokes, P. Rinke, and R. W. Godby, Phys. Rev. A **75**, 032505 (2007).
[66] F. Aryasetiawan, R. Sakuma, and K. Karlsson, Phys. Rev. B **85**, 035106 (2012).
[67] I. Ikemoto, K. Samizo, T. Fujikawa, K. Ishii, T. Ohta, and H. Kuroda, Chem. Lett. **7**, 785 (1974).
[68] D. Khuseynov, M. T. Fontana, and A. Sanov, Chem. Phys. Lett. **550**, 15 (2012).
[69] R. M. Richard, M. S. Marshall, O. Dolgounitcheva, J. V. Ortiz, J.-L. Bredas, N. Marom, C. D. Sherrill (unpublished).
[70] B. Milián, R. Pou-Amérigo, M. Merchán, and E. Ortí, ChemPhysChem **6**, 503 (2005).